Applied Mathematical Modelling 40 (2016) 1052–1068

Contents lists available at ScienceDirect

Applied Mathematical Modelling

journal homepage: www.elsevier.com/locate/apm

Boundary element method to estimate the time-varying interfacial boundary in horizontal immiscible liquids flow using electrical resistance tomography

Anil Kumar Khambampati[a], Kyung Youn Kim[b], Yeon-Gun Lee[c], Sin Kim[d,*]

[a] Institute for Nuclear Science and Technology, Jeju National University, Jeju, 690-756, Korea
[b] Department of Electronic Engineering, Jeju National University, Jeju, 690-756, Korea
[c] Department of Nuclear and Energy Engineering, Jeju National University, Jeju, 690-756, Korea
[d] School of Energy Systems Engineering, Chung-Ang University, Seoul 156-756, Korea

ARTICLE INFO

Article history:
Received 5 August 2014
Revised 4 May 2015
Accepted 17 June 2015
Available online 21 July 2015

Keywords:
Electrical resistance tomography
Boundary element method
Immiscible liquid flow
Nonlinear systems
Dynamic imaging

ABSTRACT

Flow of immiscible liquids through horizontal pipe is observed in many industrial process applications. The flow is mainly characterized by its flow regime, relative phase velocities, liquid fraction and water holdup. Electrical resistance tomography (ERT) that provides a cross-sectional image of flow distribution is helpful in monitoring the process. In this paper, the moving interfacial boundary between the immiscible liquids of stratified flow is estimated based on the measured voltages on the pipe surface. Determining the time-varying shape and location of the interfacial boundary has a practical significance. It gives us the cross-sectional liquid fraction which is a key parameter to analyze the hydrodynamic properties of flow. The interfacial boundary shape and location is parameterized with discrete front points and the forward solution is formulated using analytical boundary element method (BEM). The analytic formulation of BEM is simple with less number of unknowns therefore it is computationally efficient. Moreover, BEM discretizes the boundaries alone and is therefore appropriate choice for interfacial boundary estimation. To estimate the time-varying boundary, conventional methods that assume no change in flow distribution within the measurement time of full frame of voltage data are inadequate. Dynamic imaging methods that use one or few sets of data can improve the temporal resolution and hence they are more accurate and practical in realistic situations. Inverse problem is treated as a state estimation problem where the front points are considered as state variables and are estimated using extended Kalman filter. Numerical simulations and phantom experiments are performed to validate the performance of the proposed method.

© 2015 Elsevier Inc. All rights reserved.

1. Introduction

Immiscible liquids flow through pipe are observed in many industrial processes [1,2]. For example, transport of oil-water in petroleum industry has immiscible liquids flowing through pipelines. Monitoring the flow characteristics in pipe such as liquid fraction, phase density, relative phase velocity and interface boundary are essential for the design and safety operation of the mechanical equipment [3–5]. Low cost, non-intrusive nature and high temporal characteristics of electrical resistance

* Corresponding author: Tel: +82 2 820 5325; fax: +82 2 3280 5867.
E-mail address: sinkim@cau.ac.kr (S. Kim).

http://dx.doi.org/10.1016/j.apm.2015.06.026
S0307-904X(15)00409-6/© 2015 Elsevier Inc. All rights reserved.

tomography (ERT) makes it a popular imaging modality for process tomography applications. In ERT, voltages are measured due to the applied currents that are injected through the discretely attached electrodes on the surface of the object. Using, the current-voltage relationship, the inner resistivity/conductivity distribution is reconstructed [6]. However, ERT has poor spatial resolution and thus some prior information is often used in image reconstruction. In situation such as immiscible liquids flow, in most cases, there is prior information available about the liquids that are flowing inside the pipe. If the conductivities of these liquids are assumed to be constant and known, then the conductivity reconstruction problem will be transformed to a boundary estimation problem. The shape and location of interfacial boundary can give us information about the liquid fraction through which the relative phase velocities can be determined thus can be helpful in monitoring the transport of fluids through process pipes.

Boundary estimation problems in ERT are classified into two types; closed and open boundary. Closed boundary problem is about recovering the boundaries of inclusions that are enclosed within homogeneous background (for example, bubbles appearing in two-phase flow). In open boundary problem, the flow domain is divided into two disjoint simply connected regions that are separated by an open interfacial boundary (for example, transport of immiscible liquids in a stratified flow). For more information on closed boundary estimation with ERT, please see [7–13]. Several methods have been proposed in literature to represent the shape of an open boundary using known functions [9, 14–17]. With regard to closed boundary, if the interfacial boundary is assumed to be smooth, truncated Fourier series can be used to represent the interfacial boundary. In case, the boundary has a complex shape, higher order Fourier series is required to represent the shape. However, the coefficients of higher order Fourier series are very sensitive to noise and therefore can affect the reconstruction performance. To overcome these problems, Kim et al. [16] introduced an efficient way to represent the open boundary shape. The interfacial boundary is parameterized with discrete front points from the reference points located at the horizon. The front point method is very efficient and can represent any complex shape with fewer unknowns.

The shape reconstruction in ERT is achieved by iterating the forward and inverse problem. In forward problem, the boundary voltages are calculated for a given conductivity distribution and injected currents. The ERT forward problem is often solved using numerical methods as it is difficult to have an analytic solution in general. The analytical solution can be derived for trivial cases [18]. Boundary element method (BEM), finite element method (FEM) and finite difference method (FDM) are generally used for solving the ERT forward problem. FEM is preferred over other methods when there are several heterogeneous regions within the domain. FEM has been previously used for shape estimation problems with ERT [8–17]. In mesh based methods such as FEM the whole domain is discretized with triangular or square elements. Due to FEM discretization, many times there are situations where the anomaly or interface boundary has intersected mesh elements. For the intersected elements on the interfacial boundary, the area weighted resistivity is assigned. In situations with high conductivity contrast of immiscible fluids, such as water and air, even a small error in computation of area weighted resistivities can have a substantial effect on calculated voltages. This can cause the reconstruction performance to deteriorate. Using a very fine mesh or adaptive meshing mechanism can improve the accuracy of FEM solution. But, this leads to increase of computational burden. BEM involves discretizing the boundaries alone and solution is computed on the boundary. Therefore, it is more suited for shape estimation problems [19–23]. In [24], ERT forward problem is formulated with BEM using complete electrode model (CEM) for shape estimation problem. However, this method is computationally intensive as it needs to calculate the potential and fluxes on the interfacial boundary. An analytical computation of boundary integrals is proposed for BEM with CEM to locate anomalies in homogeneous background which is a closed boundary problem [25,26]. In [27,28], BEM is formulated for free surface and stratified flow problem to estimate the open interfacial boundary using ERT. The interfacial boundary is assumed to be stationary i.e. boundary remains unchanged during the time to collect one full frame of independent voltage measurements and the Levenberg–Marquardt method is used as an inverse algorithm for shape estimation. In real situations, the flow is very dynamic and therefore assuming the boundary is static within measurement time of full frame is not practical. Hence, dynamic techniques that consider one or few voltage data instead of full frame are necessary to estimate the time-varying interfacial boundary.

In this paper, a dynamic estimation method is devised to estimate the time-varying interfacial boundary of immiscible liquids in horizontal pipe flows. The forward problem of immiscible liquid flow is formulated using boundary element method with analytic boundary integration. As prior information, it was assumed that the conductivity of liquids is constant during the flow and their value is known thus the conductivity reconstruction problem is transformed to boundary estimation. The interfacial boundary is represented using interpolation of discrete front points. The front points are evaluated at the reference points on the horizon. The flow is considered to be rapidly varying and hence one or few sets of data are used in image reconstruction. The inverse problem is treated as state estimation problem where the front point locations are treated as state variables. The time-varying front point locations are estimated with extended Kalman filter (EKF). Using the proposed BEM with EKF approach, it is possible to estimate the moving interfacial boundary location and shape with good accuracy. Several numerical simulations and phantom experiments with 2D circular domain are performed to show the feasibility of the proposed method.

2. ERT forward problem and boundary parameterization

2.1. Problem description and physical model of ERT

Let us consider a stratified flow inside a circular pipe of radius R with two immiscible liquids (Fig. 1). The flow region Ω is divided into two distinct regions Ω_l and Ω_u whose conductivities are assumed to be known *a priori*. The immiscible liquids in the flow region are separated by an open interfacial boundary ∂D. The interfacial boundary changes rapidly with time due to the

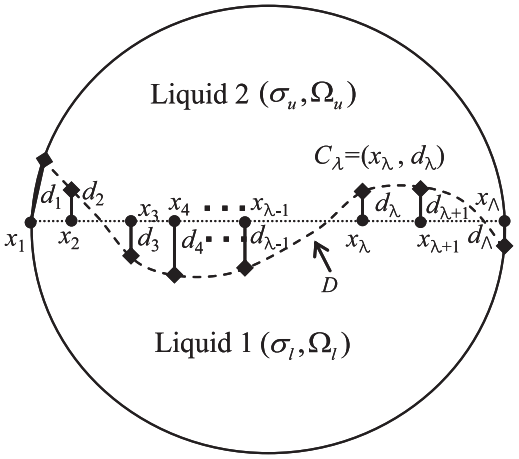


Fig. 1. Shape parameterization of interfacial boundary using discrete front point approach.

flow characteristics of immiscible liquids. The interfacial boundary is parameterized with known functions whose coefficients determine the open boundary shape and location. To monitor the flow characteristics inside a pipe using ERT, an array of L electrodes $e_\ell (\ell = 1, 2, \ldots, L)$ are attached discretely on the circumference of the pipe $\partial\Omega$. Through these L electrodes, electrical currents are injected into the flow region Ω and the resulting voltages are measured on the electrode surface. The voltage-current relationship can be used to study the flow conditions. The governing equation of ERT is a Laplace equation which is derived from Maxwell equations [6]. The governing equation gives the relationship between the potential distribution u on the flow domain Ω and the internal conductivity distribution σ which can be shown as follows

$$\nabla \cdot \sigma(p) \nabla u(p) = 0, \quad p = (x, y) \in \Omega, \tag{1}$$

where p is the spatial location within the domain Ω. The conductivity distribution $\sigma(p)$ inside the domain Ω is given by

$$\sigma(p) = \sigma_l + (\sigma_u - \sigma_l)\chi(p) \quad \text{in} \quad \Omega, \tag{2}$$

where σ_l, σ_u are the conductivities of immiscible liquids in the regions Ω_l and Ω_u, respectively. In Eq. (2), $\chi(x, y)$ is a characteristic function of region Ω_u, that is, $\chi(x, y)$ has value 1 on Ω_u and 0 otherwise. To solve for potential distribution for a given conductivity distribution, boundary conditions have to be imposed. In practice, we know the current flowing through the electrode rather than the current density. Hence, instead of the conventional current density-type boundary condition, total current injected on each electrode is considered as boundary condition and is expressed as

$$\int_{e_\ell} \sigma(p) \frac{\partial u(p)}{\partial \nu} dS = I_\ell, \quad \ell = 1, 2, \ldots, L \tag{3}$$

where I_ℓ is the electrical current injected through the ℓth electrode e_ℓ which is attached on pipe periphery $\partial\Omega$. The boundary between electrodes is insulated i.e. current density is taken as zero

$$\sigma(p) \frac{\partial u(p)}{\partial \nu} = 0 \quad \text{on} \quad \partial\Omega \setminus \cup_{\ell=1}^{L} e_\ell, \tag{4}$$

Using Eqs. (1–4), the potential distribution cannot be solved. This can have multiple solutions as addition of any constant to u will satisfy the governing equation and the boundary conditions. Also, using Eq. (3), the current density on the electrode region cannot be determined. Moreover, an electrode model is necessary that can represent the measured potential on electrodes. In here, complete electrode model (CEM) which considers the discreteness, shunting effect and effective contact impedance between electrode and the substance is used [29]. In CEM, the voltage on the ℓth electrode has the form

$$u(p) + z_\ell \sigma(p) \frac{\partial u(p)}{\partial \nu} = U_\ell, \, p \in e_\ell, \, \ell = 1, 2, \ldots, L, \tag{5}$$

where z_ℓ is the effective contact impedance between the ℓth electrode and the medium, ν is the outward unit normal vector, and U_ℓ is the measured voltage on the ℓth electrode. Rearranging Eq. (4), the current density across the electrode boundary is written as

$$\sigma(p) \frac{\partial u(p)}{\partial \nu} = \frac{1}{z_\ell} \big[U_\ell - u(p) \big], \, p \in e_\ell, \, \ell = 1, 2, \ldots, L \tag{6}$$

Substituting Eq. (6) into Eq. (2) we have

$$\frac{1}{|e_\ell|} \int_{e_\ell} u(p) dS + \frac{z_\ell I_\ell}{|e_\ell|} = U_\ell. \tag{7}$$

Now, the governing equation Eq. (1) subject to the boundary conditions Eq. (4) and Eq. (7) can be solved with known electrode currents I_ℓ. If necessary, the current density distribution can be computed by evaluating Eq. (6) after obtaining $u(p)$ and U_ℓ. If the conductivities of the immiscible liquids (σ_l, σ_u) are assumed to be known *a priori* and the conductivities are assumed to be constant within the distinct regions then the governing equation Eq. (1) reduces to

$$\nabla^2 u_l(p) = 0 \quad \text{in} \quad \Omega_l, \tag{8}$$

$$\nabla^2 u_u(p) = 0 \quad \text{in} \quad \Omega_u, \tag{9}$$

where u_l and u_u are the potentials in the region Ω_l and Ω_u, respectively. The current densities and the potential distribution should be continuous at the interfacial boundary ∂D, therefore we have an interfacial boundary condition as

$$\sigma_l \frac{\partial u_l}{\partial \nu} = \sigma_u \frac{\partial u_u}{\partial \nu} \quad \text{and} \quad u_l = u_u \quad \text{on} \quad \partial D. \tag{10}$$

Apart from the boundary conditions and interfacial condition, additional constraint is needed to have a unique solution [30]

$$\sum_{\ell=1}^{L} I_\ell = 0 \quad \text{and} \quad \sum_{\ell=1}^{L} U_\ell = 0. \tag{11}$$

The outer boundary of circular pipe $\partial\Omega$ consists of electrode and gap boundaries represented as $\partial\Omega = \partial\Omega_E \cup \partial\Omega_G$, $\partial\Omega_E = \cup_{\ell=1}^{L} e_\ell$, $\partial\Omega_G = \cup_{\ell=1}^{L} g_\ell$. Here, e_ℓ and g_ℓ are the boundary segments of electrode and gap, respectively.

2.2. Boundary parameterization of open interfacial boundary

Let us assume that there is prior knowledge available about the constituents and their conductivity values of immiscible liquids flowing through horizontal pipe. With the conductivity of constituent liquids is known and constant during the flow, the unknowns are the parameters that describe the location and shape of the interfacial boundary. The open interfacial boundary can be parameterized with discrete front points C_λ, $\lambda = 1, 2, \ldots, \Lambda$ such that the interpolation of the front points represents the shape of the interfacial boundary ∂D [16]. Therefore, the interfacial boundary formed by interpolation of front points is piecewise continuous and can be represented as

$$\partial D(x) = \sum_{\lambda=2}^{\Lambda} S_\lambda(x)\, \chi(x, X_{\lambda-1}, X_\lambda), \quad x \in [X_1, X_\Lambda], \tag{12}$$

where

$$S_\lambda(x) = \frac{Y_\lambda - Y_{\lambda-1}}{X_\lambda - X_{\lambda-1}}(x - X_{\lambda-1}) + Y_{\lambda-1}, \quad \lambda = 2, \ldots, \Lambda, \tag{13}$$

and $\chi(x, X_{\lambda-1}, X_\lambda)$ is a unit pulse defined for $x \in [X_{\lambda-1}, X_\lambda]$. Here, (X_λ, Y_λ) are the coordinates for front points C_λ on the interfacial boundary ∂D and Λ is the total number of front points that are used to describe the interfacial boundary. C_1 and C_Λ are the leftmost and the rightmost front points, respectively. The location of front points C_λ on the interfacial boundary are represented as $(X_\lambda, Y_\lambda) = (x_\lambda, d_\lambda)$, where x_λ are the reference points located at the central horizon which are known *a priori* and d_λ is the vertical distance from the known reference point to the front point on the boundary (Fig. 1). The front points are therefore dependent on the variable d_λ. Therefore, excluding the end front points, the intermediate front points ($\lambda = 2, \ldots, \Lambda - 1$) are denoted by the vertical distance d_λ from the given reference point x_λ. The front point location $C_\lambda = (x_\lambda, d_\lambda)$ on the interface are represented as

$$(X_\lambda, Y_\lambda) = (x_\lambda, d_\lambda), \quad \lambda = 2, \ldots, \Lambda - 1, \tag{14}$$

To limit the boundary within the circumference of the pipe, the end points are characterized by the arc length

$$(X_1, Y_1) = \left(-R\cos\frac{d_1}{R}, R\sin\frac{d_1}{R}\right), \tag{15}$$

$$(X_\Lambda, Y_\Lambda) = \left(R\cos\frac{d_\Lambda}{R}, R\sin\frac{d_\Lambda}{R}\right). \tag{16}$$

Moreover, the intermediate front points are subjected to constraint such that the front points stay within the domain surface $\partial\Omega$. The unknown parameters to be estimated are the front point variables given by

$$d = d_1, d_2, \ldots, d_\Lambda \in \Re^\Lambda \tag{17}$$

2.3. BEM solution for immiscible liquid flow

The primary objective is to estimate the unknown front points location using the measured boundary voltages. In here, the ERT forward problem to compute the boundary voltages is formulated using boundary element method (BEM). BEM is formulated by integrating the fundamental solution of Laplace equation over the domain boundary. The fundamental solution of Laplace equation and its derivatives in 2D are of the form [25, 31]

$$G(p|p_s) = \frac{1}{2\pi}\ln|p-p_s|, \tag{18}$$

$$Q(p|p_s) = \frac{\partial G(p|p_s)}{\partial \nu} = \frac{1}{2\pi|p-p_s|}\frac{\partial|p-p_s|}{\partial \nu} = \frac{(p-p_s)\cdot\nu}{2\pi|p-p_s|^2}, \tag{19}$$

where p and p_s are the field and source point, respectively. Considering the conductivities are constant within the distinct regions separated by an interfacial boundary and using Green–Gauss theorem for regions Ω_u and Ω_l results in the following equations for lower and upper regions i.e.

$$\begin{aligned}\omega_l u_l(p_s) = &\int_{\partial\Omega_l} u_l(p)Q_l(p|p_s)dS + \int_{\partial D} u_l(p)Q_l(p|p_s)dS \\ &- \int_{\partial\Omega_l} G(p|p_s)\frac{\partial u_l(p)}{\partial \nu_l}dS - \int_{\partial D} G(p|p_s)\frac{\partial u_l(p)}{\partial \nu_l}dS \quad \text{in} \quad p_s \in \bar{\Omega}_l,\end{aligned} \tag{20}$$

$$\begin{aligned}\omega_u u_u(p_s) = &\int_{\partial\Omega_u} u_u(p)Q_u(p|p_s)dS + \int_{\partial D} u_u(p)Q_u(p|p_s)dS \\ &- \int_{\partial\Omega_u} G(p|p_s)\frac{\partial u_u(p)}{\partial \nu_u}dS - \int_{\partial D} G(p|p_s)\frac{\partial u_u(p)}{\partial \nu_u}dS \quad \text{in} \quad p_s \in \bar{\Omega}_u\end{aligned} \tag{21}$$

where $\bar{\Omega}_l = \Omega_l \cup \partial D$, $\bar{\Omega}_u = \Omega_u \cup \partial D$ represents the upper and lower regions with the interfacial boundary closure. In Eqs. (20) and (21), ω_l and ω_u are the geometric coefficients defined on the discretized boundary points on lower and upper regions. The geometric coefficient is determined by considering the internal angle at discretized point divided by 2π. Considering the interfacial condition Eq. (10), Eq. (21) is rewritten as

$$\begin{aligned}\kappa\omega_u u_u(p_s) = &\kappa\int_{\partial\Omega_u} u_u(p)Q_u(p|p_s)dS - \kappa\int_{\partial D} u_l(p)Q_l(p|p_s)dS \\ &- \kappa\int_{\partial\Omega_u} G(p|p_s)\frac{\partial u_u(p)}{\partial \nu_u}dS + \int_{\partial D} G(p|p_s)\frac{\partial u_l(p)}{\partial \nu_l}dS \quad \text{in} \quad p_s \in \bar{\Omega}_u\end{aligned} \tag{22}$$

where $\kappa = \sigma_u/\sigma_l$. Note that on ∂D the outward unit normal from Ω_l is opposite to that from Ω_u. Combining Eq. (20) and Eq. (22) we have

$$\begin{aligned}\omega' u'(p_s) = &\int_{\partial\Omega_l} u_l(p)Q_l(p|p_s)dS + \kappa\int_{\partial\Omega_u} u_u(p)Q_u(p|p_s)dS \\ &+ (1-\kappa)\int_{\partial D} u_l(p)Q_l(p|p_s)dS - \int_{\partial\Omega_l} G(p|p_s)\frac{\partial u_l(p)}{\partial \nu_l}dS \quad \text{in} \quad p_s \in \overline{\Omega} \\ &- \kappa\int_{\partial\Omega_u} G(p|p_s)\frac{\partial u_u(p)}{\partial \nu_u}dS\end{aligned} \tag{23}$$

where

$$\omega' u' = \begin{cases}\omega_l u_l \ in \ p_s \in \partial\Omega_l \\ \kappa\omega_u u_u \ in \ p_s \in \partial\Omega_u \\ \omega_l u_l + \kappa\omega_u u_u \ in \ p_s \in \partial D\end{cases} \tag{24}$$

Introducing the complete electrode model into Eq. (23), we have

$$\begin{aligned}\omega' u'(p_s) = &\int_{\partial\Omega_l} u_l(p)Q_l(p|p_s)dS + \kappa\int_{\partial\Omega_u} u_u(p)Q_u(p|p_s)dS + (1-\kappa)\int_{\partial D} u_l(p)Q_l(p|p_s)dS \\ &- \sum_{\ell=1}^{L_l}\int_{e_\ell} G(p|p_s)\frac{U_\ell - u_l(p)}{z_\ell\sigma_l(p)}dS - \kappa\sum_{\ell=1}^{L_u}\int_{e_\ell} G(p|p_s)\frac{U_\ell - u_u(p)}{z_\ell\sigma_u(p)}dS\end{aligned} \tag{25}$$

where L_l and L_u are the number of electrodes present in $\partial\Omega_l$ and $\partial\Omega_u$, respectively. The segments on the electrode, gap and interfacial boundary are defined as follows

$$M_{Eu} = \sum_{\ell=1}^{L_u} M_e(\ell), \quad M_{El} = \sum_{\ell=1}^{L_l} M_e(\ell), \quad M_E = M_{Eu} + M_{El}, \tag{26}$$

$$M_{Gu} = \sum_{\ell=1}^{L_u} M_g(\ell), \quad M_{Gl} = \sum_{\ell=1}^{L_l} M_g(\ell), \quad M_G = M_{Gu} + M_{Gl}, \tag{27}$$

$$M_B = M_E + M_G, \quad M_A = \sum_{n=1}^{\Lambda} M_a(n), \quad M = M_B + M_A, \tag{28}$$

$$e_\ell = \cup_{m=1}^{M_e(\ell)} e_{\ell,m}, \quad g_\ell = \cup_{m=1}^{M_g(\ell)} g_{\ell,m}. \tag{29}$$

The formulation in Eq. (25) is for the case when interfacial boundary does not intersect the electrode surface. However, during the flow process, there can be a situation where interfacial boundary contains part or whole part of electrode area. Let us suppose the electrode L_D contains interfacial boundary ∂D such that M_d segments of electrode lie in lower region Ω_l and remaining $(M_e - M_d)$ segments lie in upper region Ω_u. The Eq. (25) will be modified as

$$\begin{aligned}\omega' u'(p_s) = &\int_{\partial\Omega_l} u_l(p) Q_l(p|p_s) dS + \kappa \int_{\partial\Omega_u} u_u(p) Q_u(p|p_s) dS + (1-\kappa) \int_{\partial D} u_l(p) Q_l(p|p_s) dS \\ &- \sum_{\ell=1}^{L_l} \int_{e_\ell} G(p|p_s) \frac{U_\ell - u_l(p)}{z_\ell \sigma_l(p)} dS - \kappa \sum_{\ell=1}^{L_u} \int_{e_\ell} G(p|p_s) \frac{U_\ell - u_u(p)}{z_\ell \sigma_u(p)} dS \\ &- \sum_{m'=1}^{M_d} \int_{e_{L_{D,m'}}} G(p|p_s) \frac{U_\ell - u_l(p)}{z_\ell \sigma_l(p)} dS - \kappa \sum_{m'=M_d+1}^{M_e - M_d} \int_{e_{L_{D,m'}}} G(p|p_s) \frac{U_\ell - u_u(p)}{z_\ell \sigma_u(p)} dS \end{aligned} \tag{30}$$

The formulation given in Eq. (25) and Eq. (30) are derived based on the end front points (C_1,C_λ) of the interfacial boundary. During the evolution of interfacial boundary, depending on the location of the end front points, the formulation given in Eq. (25) and Eq. (30) is chosen automatically.

From CEM, the voltages measured on the electrodes can be written as

$$\frac{1}{|e_\ell|} \int_{e_\ell} u(p) dS + \frac{z_\ell I_\ell}{|e_\ell|} = U_\ell. \tag{31}$$

If the potential $u(p)$ is assumed to be constant within each segment of $\partial\Omega$ and ∂D, the forward solution can be expressed as a set of linear algebraic equations in a matrix form as

$$D(\omega) \begin{bmatrix} u_E \\ u_G \\ u_A \end{bmatrix} - \begin{bmatrix} K_E & K_G & (1-\kappa) K_A \end{bmatrix} \begin{bmatrix} u_E \\ u_G \\ u_A \end{bmatrix} + K_U U = 0 \tag{32}$$

$$U = A u_E + D(z_\ell / |e_\ell|) \tilde{I} = A u_E + U_d \tag{33}$$

where

$$D(\omega) = diag(\omega_1, \omega_2, \ldots, \omega_M) \in \Re^{M \times M}, \tag{34}$$

$$u_E = \begin{bmatrix} u_1 & u_2 & \ldots. & u_{M_E} \end{bmatrix}^T \in \Re^{M_E}, \tag{35}$$

$$u_G = \begin{bmatrix} u_{M_E+1} & u_{M_E+2} & \ldots & u_{M_E+M_G} \end{bmatrix}^T \in \Re^{M_G}, \tag{36}$$

$$u_A = \begin{bmatrix} u_{M_B+1} & u_{M_B+2} & \ldots & u_{M_B+M_A} \end{bmatrix}^T \in \Re^{M_A}, \tag{37}$$

$$\tilde{I} = [I_1 \quad I_2 \quad \ldots \quad I_L] \in \Re^{L \times 1}, \tag{38}$$

$$Q_{El}(i,j) = \int_{\partial\Omega_{El_j}} Q(p|p_i) dS \in \Re^{M \times M_{El}}, \quad Q_{Eu}(i,j) = \int_{\partial\Omega_{E_{uj}}} Q(p|p_i) dS \in \Re^{M \times M_{Eu}}, \tag{39}$$

$$G_{El}(i,j) = \int_{\partial\Omega_{El_j}} G(p|p_i) dS \in \Re^{M \times M_{El}}, \quad G_{Eu}(i,j) = \int_{\partial\Omega_{Eu_j}} G(p|p_i) dS \in \Re^{M \times M_{Eu}} \tag{40}$$

$$K_{El} = Q_{El} + \frac{1}{\sigma_l(p)} G_{El} \left[D(1/z_l) \otimes I_{m_{El}} \right] \in \Re^{M \times M_{El}}, \tag{41}$$

$$K_{Eu} = Q_{Eu} + \frac{1}{\sigma_u(p)} G_{Eu} \left[D(1/z_l) \otimes I_{m_{Eu}} \right] \in \Re^{M \times M_{Eu}}, \tag{42}$$

$$K_{Gl}(i,j) = \int_{\partial\Omega_{G_j}} Q(p|p_i) dS \in \Re^{M \times M_{Gl}}, \tag{43}$$

$$K_{Gu}(i,j) = \int_{\partial\Omega_{G_j}} Q(p|p_i)dS \in \Re^{M\times M_{Gu}}, \tag{44}$$

$$K_A(i,j) = \int_{\partial D_j} Q(p|p_i)dS \in \Re^{M\times M_A}, \tag{45}$$

$$K_U = \frac{1}{\sigma_b} G_E\left[D(1/z_l)\otimes \text{ones}(m_E,1)\right] \in \Re^{M\times L}, \tag{46}$$

$$U = \begin{bmatrix} U_1 & U_2 & \cdots & U_L \end{bmatrix}^T \in \Re^L, \tag{47}$$

$$A = \frac{s_E}{|e|} I_L \otimes \text{ones}(1, m_E) \in \Re^{L\times M_E}, \tag{48}$$

$$D(z_\ell/|e_\ell|) = \text{diag}(z_1/|e_1| \quad z_2/|e_2| \quad \ldots \quad z_L/|e_L|) \in \Re^{L\times L} \tag{49}$$

In this, $\otimes$ denotes the Kronecker matrix product, $I_{M_{El}} \in \Re^{M_{El}\times M_{El}}$ the identity matrix, and ones(m, n) the m-by-n matrix with ones. The forward solution given in Eqs. (32) and (33) is not unique. To ensure the uniqueness of the solution, constraint Eq. (11) is used. Therefore, the forward solution given in Eqs. (32) and (33) is modified as

$$\left[D(\omega) - K\right]u = -K_U \tilde{N} D(z_\ell/|e_\ell|)\tilde{I}, \tag{50}$$

$$U = Au_E + D(z_\ell/|e_\ell|)\tilde{I}, \tag{51}$$

where

$$K = \begin{bmatrix} K_E - K_U\tilde{N}A & K_G & (1-\kappa)K_A \end{bmatrix}, \tag{52}$$

$$u = [u_E \quad u_G \quad u_A]^T, \tag{53}$$

$$N_U = \left[\text{ones}(1, L-1); -I_{L-1}\right], \tag{54}$$

$$\tilde{N} = N_U\left(N_U^T N_U\right)^{-1} N_U^T. \tag{55}$$

The boundary integrals in Eqs. (39–45) are computed analytically by discretizing the outer boundary into points to form line segments of constant element [25, 31–36]. The potential and its derivates are computed at the midpoint of the line segment and are assumed to be constant over the line segment [22].

3. Inverse problem: dynamic interfacial boundary estimation

In this section, we provide the procedure to estimate immiscible liquids interfacial boundary shape and location from the measured boundary voltages and injected currents. To deal with the fast changes in the flow due to which the boundary parameters change swiftly, we need to adopt a dynamic estimation approach. The underlying inverse problem is modelled using state estimation approach. The state estimation problem constitutes of state equation and observation equation. State equation is used to model the temporal evolution of the state variable whereas the observation equation relates the state variable and the measurement parameters. In here, the state variables are the front point parameters d that characterize the shape of interfacial boundary. The measurements are the boundary voltages that are recorded on the surface of the electrodes.

3.1. Extended Kalman filter for front point estimation

Assuming that the evolution of the state variables is smooth, the dynamic equation is modelled by a stochastic linear difference equation given by [8, 37]

$$d_k = F_{k-1}d_{k-1} + w_{k-1}, \tag{56}$$

and the measurement equation in ERT for measured voltages $V \in \Re^{L\times k}$ is of the form

$$V_k = U_k(d_k) + v_k, \tag{57}$$

where the subscript k is the time index, $F_k \in \Re^{\Lambda\times\Lambda}$ is the state transition model, $U_k(d_k)$ is the forward solution computed from BEM, V_k is the vector of voltages measured at time step k and L is the number of measurement electrodes. The random variables $w_k \in \Re^\Lambda$ and $v_k \in \Re^L$ correspond to process and the measurement noise, respectively. The process and measurement noise are assumed to be independent and zero-mean normally distributed random variables with known covariance matrices $\bar{Q}_k \in \Re^{\Lambda\times\Lambda}$ and $\bar{R}_k \in \Re^{L\times L}$ i.e.

$$p(w_k) \sim N(0, \bar{Q}_k), \tag{58}$$

$$p(v_k) \sim N(0, \bar{R}_k). \tag{59}$$

The above Eqs. (56–59) constitute the state-space representation for the ERT shape estimation problem. The observation equation in ERT is nonlinear therefore the conditional expectations $d_{k|k}$ are determined using extended Kalman filter (EKF). In EKF, the state variables d_k are estimated from the measurements recorded up to the time kT, where T is the total time of measurement [37]. EKF is formulated by minimizing the cost function derived from the state-space model with Gaussian assumption. The cost functional for shape estimation problem in ERT with EKF is of the form

$$\Phi(d_k) = \frac{\alpha}{2}\left\{ \left\| R(d_k - d_{k|k-1}) \right\|^2_{P^{-1}_{k|k-1}} + \left\| V_k - J(d_{k|k-1})d_k \right\|^2_{R^{-1}_k} \right\}, \tag{60}$$

where $\|x\|_\Lambda$ denotes $x^T\Lambda x$, α is the regularization parameter, R is the regularization martix, J is the Jacobian matrix, $P_{k|k-1}$ is the time-updated error covariance matrix defined as

$$P_{k|k-1} = E\left[(d_k - d_{k|k-1})(d_k - d_{k|k-1})^T \right]. \tag{61}$$

Minimizing the cost functional Eq. (60) and solving for the updates of the associated covariance matrices, recursive EKF algorithm is obtained, which consists of prediction and filtering steps [8, 26,37]

Prediction:

$$d_{k|k-1} = F_{k-1}d_{k-1|k-1}. \tag{62}$$

$$P_{k|k-1} = F_{k-1}P_{k-1|k-1}F^T_{k-1} + \bar{Q}_{k-1}. \tag{63}$$

Filtering:

$$\varepsilon_k = V_k - U(d_{k|k-1}). \tag{64}$$

$$S_k = \mathrm{COV}(\varepsilon_k) = J_k P_{k|k-1} {J_k}^T + \bar{R}_k. \tag{65}$$

$$K_k = P_{k|k-1}J_K {S_k}^{-1}. \tag{66}$$

$$d_{k|k} = d_{k|k-1} + K_k\varepsilon_k = d_{k|k-1} + K_k(V_k - J_k(d_{k|k-1})). \tag{67}$$

$$P_{k|k} = (I - K_kJ_k)P_{k|k-1}. \tag{68}$$

where J_k represents the Jacobian with respect to previous state $d_{k|k-1}$. The Jacobian matrix is computed using perturbation method where each front point variable d_λ is perturbed in turn by a small value say epsilon and the relative change in voltage with respect to change in front variable is evaluated for approxmiation of Jacobian. With the initial guess for front point parameters $d_{0|0}$, error covariance $P_{0|0}$ and the associated process noise covariance $\bar{Q}_0$ the predicted parameters $d_{1|0}$, $P_{1|0}$ are computed using Eqs. (62) and (63) and the predicted values are corrected from the measured voltage data V_1 to get the posterior data $d_{1|1}$, $P_{1|1}$. The process is carried for all time steps such that the state variables d_k are estimated during the measurement time T.

4. Results and discussion

4.1. Numerical results

In this section, we present the reconstructed numerical results for interfacial boundary of stratified immiscible liquids using proposed method. A cylindrical pipe of radius 4 cm containing stratified flow of two immiscible liquids is considered for numerical simulation. The flow region is separated into distinct regions with liquids separated by an open interfacial boundary. The conductivities of the liquids are assumed to be constant and known *a priori* and therefore the problem becomes the estimation of shape and location of the interfacial boundary. The lower region has water as liquid and the upper region is filled with liquid that has lower conductivity compared to water. Along the circumference of the pipe, 16 electrodes with width 0.6 cm and height 20 cm are attached. This is a two dimensional imaging as the electrodes span the entire length of the ERT sensor. Opposite method is used as a current injection method i.e. electrodes that are located inline are used as source and sink while others are insulated. Current of amplitude 1 mA is applied through the electrodes attached on the pipe circumference and the resulting excited voltages are measured.

To verify the accuracy of computed BEM solution, homogeneous conditions are assumed in flow domain such that the pipeline is filled with water that has conductivity of 0.003 S/cm. The computed forward voltages are compared against analytical solution and FEM solution using complete electrode model (Fig. 2(a)). Analytical solution is computed with 1024 Fourier coefficients and FEM solution is obtained from mesh that has 11 456 elements. From Fig. 2(a) it can be noticed that the boundary voltages computed with BEM are in good agreement with analytical and FEM solution. Also, relative error of BEM with respected to number of segments is computed with respect to analytical solution and the results are shown in Fig. 2(b). It can be seen that BEM solution accuracy is improved as the number of segments is increased. Moreover, BEM solution with 10 or more segments on the electrode and gap has relative error less than 0.5%. Therefore, in numerical simulation for BEM, outer boundary discretized with 10 segments on each electrode and gap region is chosen. Also, it is to be understood that the computation time of BEM using

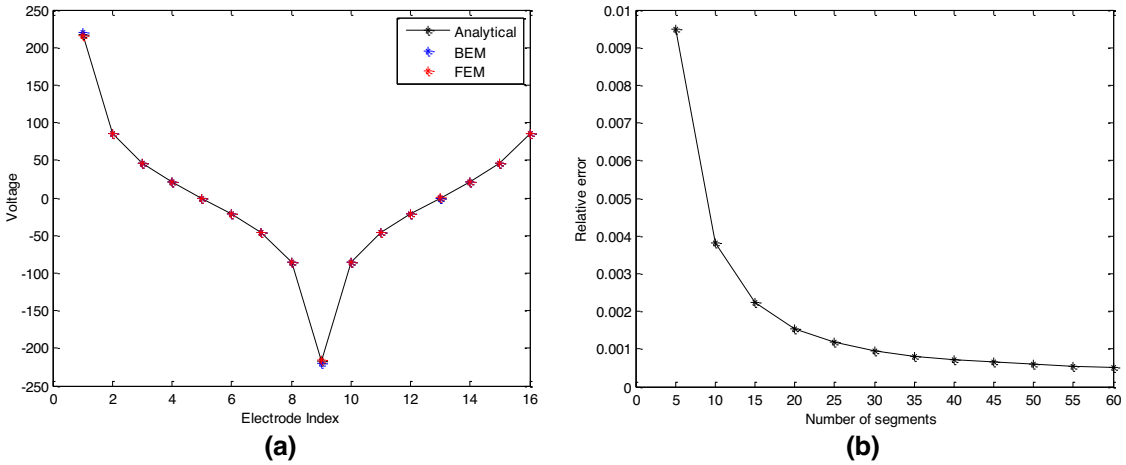


Fig. 2. Evaluation of computed BEM solution with respect to homogenous condition (a) comparison of computed forward solution of BEM with analytic and FEM solution (b) relative error of BEM with respect to number of segments on electrode and gap.

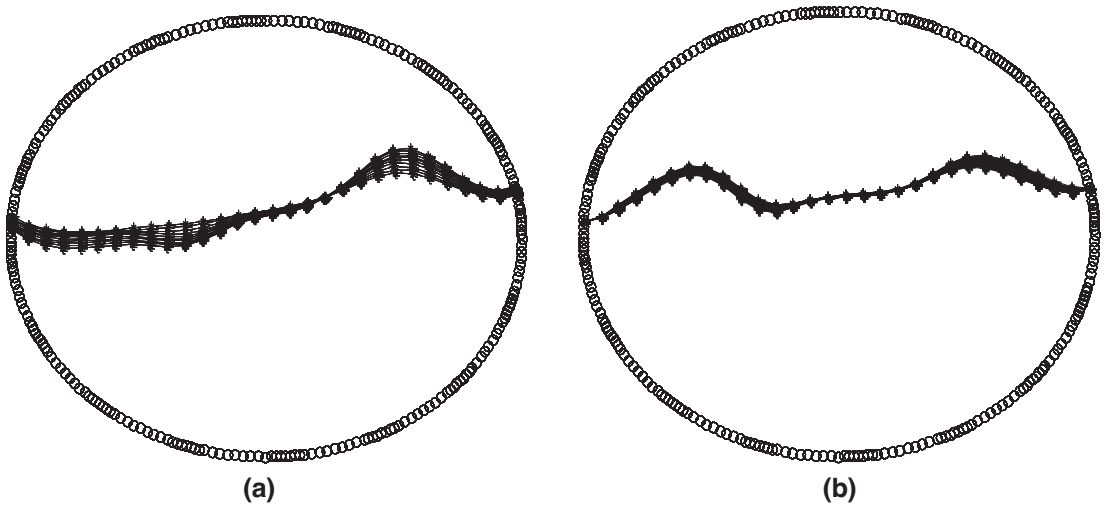


Fig. 3. Numerical scenarios considered for moving interfacial boundary estimation (a) scenario 1 (b) Scenario 2.

10 segments on electrode and gap regions is less as compared to FEM solution with 11,456 elements and also BEM has better accuracy.

Dynamic interfacial boundary estimation is simulated by considering the interfacial boundary between immiscible liquids to be non-stationary within the time to measure one frame of voltage data. Two different scenarios are considered where the interfacial boundary evolves inside the flow domain with different temporal resolution (Fig. 3). Scenario 1 initially has the interfacial boundary located near to the center of the pipe and has a smooth surface with the front points at the right side of the boundary are more perturbed compared to left end points. With time, the interface changes its position and evolves such that the left end points on the boundary trails to lower region where as the right end front points transcends to upper region resulting in hump like structure at the right side of the interface. The interface changes its position within the time to acquire four current patterns i.e. the interface change two times within the time to acquire one full frame of data. Therefore, the temporal resolution is increased by two times as compared to static imaging. A total of five data frames i.e. (40 current injections) are considered in the generation of scenario 1 where the interface evolves inside the pipe as given in Fig. 3(a). In EKF, one or few voltage data sets corresponding to injected current injection patterns are used. Therefore, the number of iterations depends on the number of independent voltage data sets that are collected during the visualization process. If the mesh structure to generate the simulated electrode voltage data is used in the ERT image reconstruction then the numerical error may be cancelled out, inadvertently. This is called the inverse crime. In order to avoid such circumstance, different number of discretization points is used in computation of forward and inverse problem. In BEM implementation, for generating the true voltage data, the outer boundary is discretized with 320 elements (10 elements on each electrode and gap). In the inverse computation, to avoid inverse crime, 256 elements (8 elements on electrode and gap) are considered on the outer boundary. In real situations there is noise involved due to the use of

Table 1
Parameters used in EKF for scenario 1.

Parameters	0.5% absolute noise				
	$\kappa = 0.2$	$\kappa = 0.05$	$\kappa = 0.0167$	$\kappa = 0.01$	$\kappa = 0.001$
F	I_{15}	I_{15}	I_{15}	I_{15}	I_{15}
$\overline{Q}$	$0.003\, I_{15}$	$0.001\, I_{15}$	$0.0005\, I_{15}$	$0.001\, I_{15}$	$0.0005\, I_{15}$
$\overline{R}$	$1 \times 10^3 I_L$	$3 \times 10^3 I_L$	$2 \times 10^4 I_L$	$7 \times 10^4 I_L$	$5 \times 10^6 I_L$
$P_{0\|0}$	$0.01\, I_{15}$	$0.05\, I_{15}$	$0.01\, I_{15}$	$0.05\, I_{15}$	$0.01\, I_{15}$

Table 2
Parameters used in EKF for scenario 2.

Parameters	0.5 % absolute noise				
	$\kappa = 0.2$	$\kappa = 0.05$	$\kappa = 0.0167$	$\kappa = 0.01$	$\kappa = 0.001$
F	I_{15}	I_{15}	I_{15}	I_{15}	I_{15}
$\overline{Q}$	$0.01\, I_{15}$	$0.0008\, I_{15}$	$0.001\, I_{15}$	$0.0009\, I_{15}$	$0.0005\, I_{15}$
$\overline{R}$	$1 \times 10^3 I_L$	$5 \times 10^3 I_L$	$4 \times 10^4 I_L$	$6 \times 10^4 I_L$	$5 \times 10^6 I_L$
$P_{0\|0}$	$0.01\, I_{15}$	$0.01\, I_{15}$	$0.01\, I_{15}$	$0.01\, I_{15}$	$0.01\, I_{15}$

electrical and mechanical equipment. Usually, the noise that is associated with the measurements is absolute noise. Therefore, in numerical simulations, 0.5% of maximum voltage measured is added to the generated voltages to depict the real situations. The conductivity contrast between the liquids is set to 20, i.e. $\kappa = 0.05$. The actual boundary is represented with 30 front points with cubic-spline to have a smooth surface. In inverse solution, choosing an appropriate initial guess is essential to have an acceptable solution. It was found that for a given conductivity contrast and pipe geometry, the measured voltages are dependent on the location of interfacial boundary. The interface is assumed to be flat and the position is varied from top to bottom of the pipe and the corresponding voltages are measured beforehand. From the measured voltages from the simulation, it is possible to determine the approximate location of the interfacial boundary from the voltage-interface location relationship. In the inverse boundary estimation, same approach is applied to determine the initial location of the boundary.

The reconstructed result for moving interfacial boundary for scenario 1 with conductivity contrast 20 is shown in Fig. 4. As there is no prior information about the boundary shape, in the reconstruction procedure 15 front points are assumed to represent the boundary shape. It can be noticed from Fig. 4 that the proposed method could track the shape and location of actual boundary with good accuracy. The number of front points considered in boundary parameterization affects the estimation of boundary shape. Fig. 5 shows the reconstruction performance of proposed method with different number of front points considered in boundary parameterization. From Fig. 5, it can be noticed that with very less number of front points ($\Lambda = 5$) and wavy interface there is more discrepancy observed between true and estimated boundary. This is due to the fact that linear interpolation used for boundary representation in inverse solution. As the number of front points is increased the reconstruction is found to improve. However, when higher number of front points ($\Lambda = 30$) are used then fluctuations among the neighbouring front points at the centre is observed. It can be found that the performance is best with 15 front points. It is found that the performance is improved as the number of front points is increased but higher number of front points can lead to increase in computational time. Moreover, with higher number of front points the performance may be affected due to ill-conditioned nature of ERT problem.

The reconstruction performance with different conductivity contrast between liquids in scenario 1 is analyzed and shown in Fig. 6. It is seen that RMSE of boundary coefficients in higher contrast ratios is less than 0.5%. The boundary is reconstructed with good accuracy and therefore it is predicted that the proposed method is suitable for monitoring liquids with higher conductivity contrast such as oil-water flow which is observed in petroleum industry. The parameters used in EKF for scenario 1 with different conductivity contrast are given in Table 1.

In scenario 2, the flow is assumed to be very fast transient such that the interfacial boundary is more fluctuating. Actual interfacial boundary is initially located at the center with all the front points perturbed randomly. With time, the interface evolves in such a way that it forms two humps as seen in Fig. 3(b). The boundary changes for every current pattern and therefore the temporal resolution is increased by 8 times compared to static imaging. Furthermore, for generating the scenario 2, total of five frames are considered such that interfacial boundary changes 40 times during the measurement time. Reconstructed results for scenario 2 with conductivity contrast 20 are shown in Fig. 7. As there are many reconstructed images (40) in scenario 2, images reconstructed after every four current patterns are shown in Fig. 7. The proposed method has estimated the complex boundary shape in scenario 2 with good accuracy. The sensitivity of proposed method with change in number of front points in inverse solution is shown in Fig. 8. It can be seen that the estimation performance is found to improve as the number of front points are increased. Finally, scenario 2 is simulated considering different conductivity contrast of immiscible liquids and performance of the proposed method is analyzed in Fig. 9. The parameter setting for EKF in reconstructing the boundary results for scenario 2 are given in Table 2. It is seen that the proposed method has good estimation performance in high transient flow conditions.

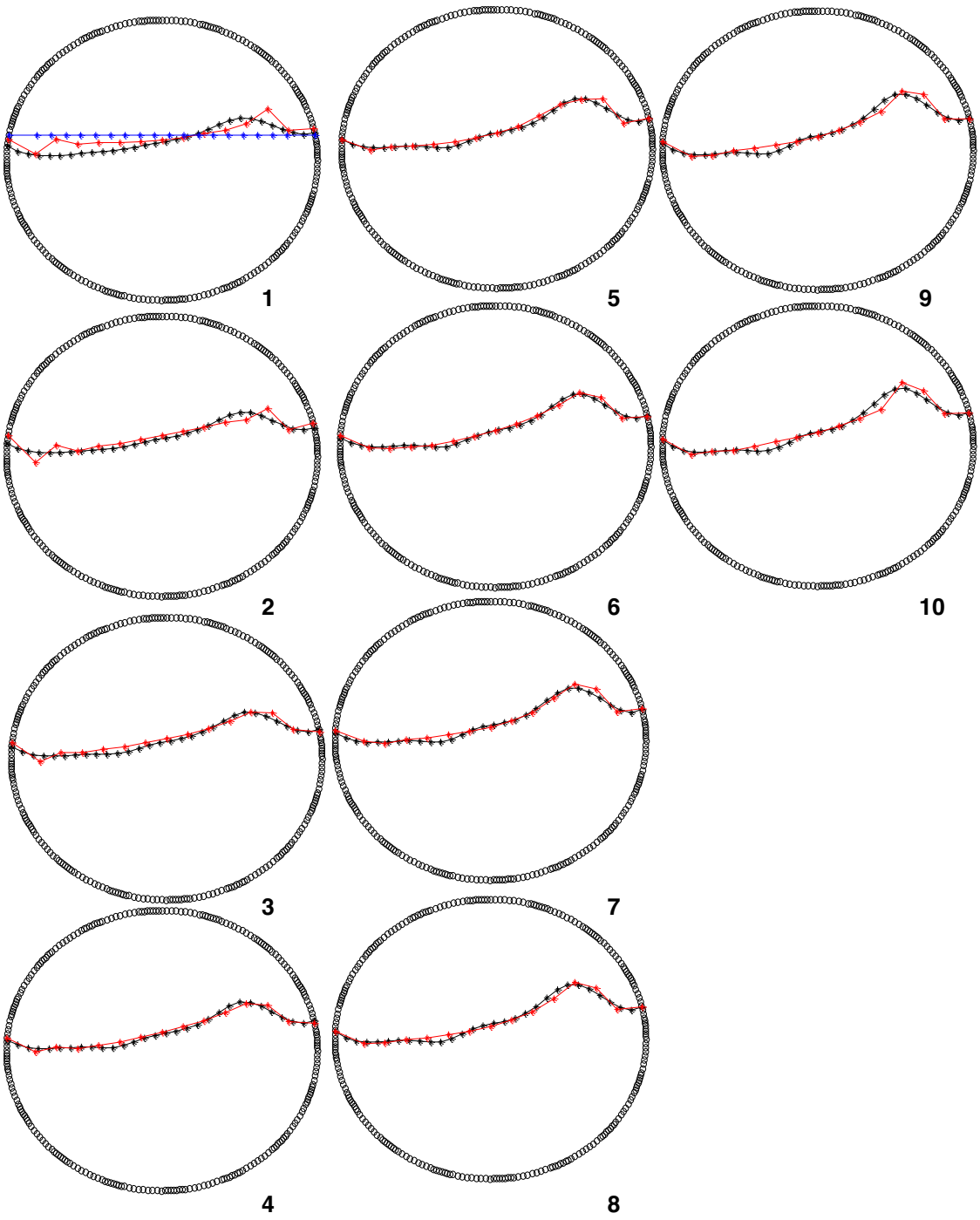


Fig. 4. Reconstructed moving interfacial boundary results with conductivity contrast 20 for numerical scenario 1. The solid black line represents the location and shape of actual boundary. The solid blue line represents the initial guess used in EKF method. The solid red line is the estimated result with proposed BEM with EKF.

From the numerical simulations it can be inferred that the proposed BEM with EKF can estimate the complex shape and location of the moving interfacial boundary. Also, it can be realized that the proposed method can be applicable to both low as well as high conductivity contrast liquids and therefore it can be applied to wide range of applications involving immiscible liquids. The reconstruction performance is affected by the number of front points used in inverse solution. More number of front points improves the shape reconstruction. However, when large number of front points is used for boundary parameterization,

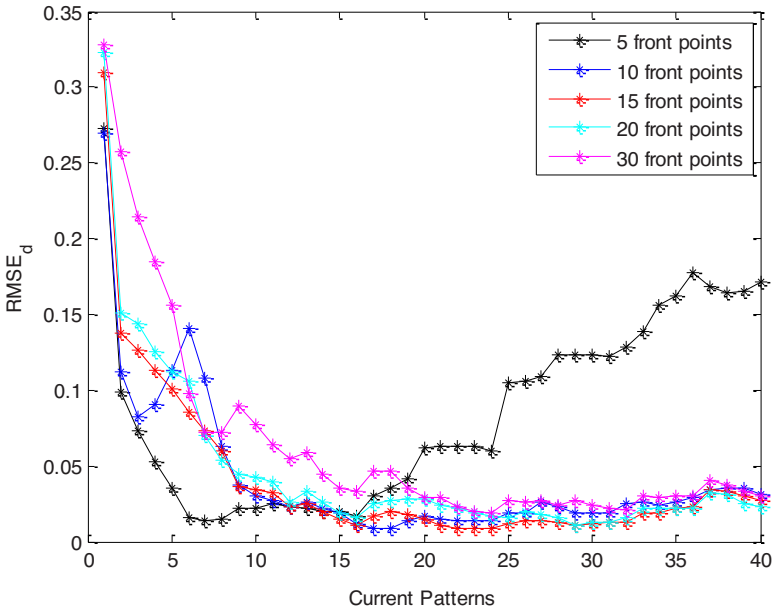


Fig. 5. Reconstruction performance of proposed method with respect to number of front points for numerical scenario 1 having conductivity contrast 20.

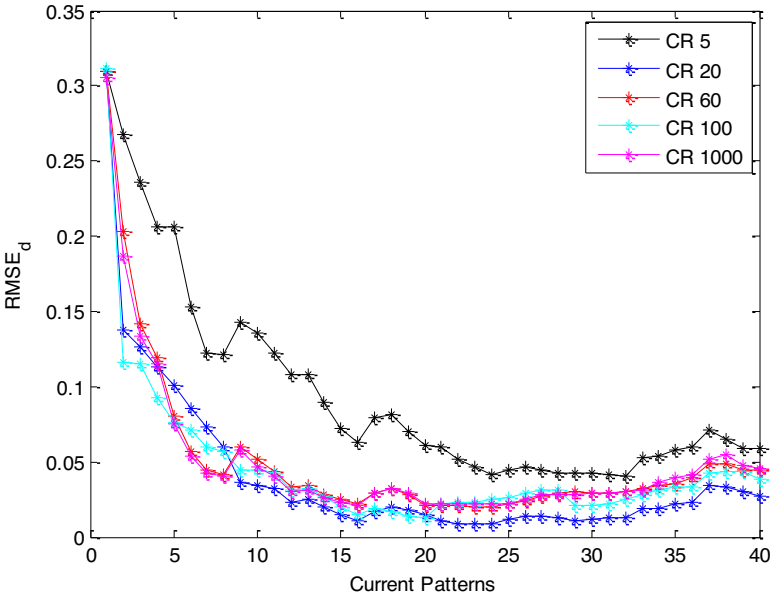


Fig. 6. Reconstruction performance of proposed method in scenario 1 having different conductivity contrast between immiscible liquids.

the neighbouring estimated front points at the centre of the domain are found to have oscillation. Hence, there should be trade off with respect to the number of the front points used to describe the boundary surface, computation time and accuracy.

4.2. Experimental results

Laboratory experiments are performed for interfacial boundary estimation with gelatine and brine solution modelled as immiscible liquids. A circular phantom with a radius of 10 cm and height 2 cm is considered for experiment. The phantom has 32 electrodes each of width 1.5 cm discretely attached around its periphery. In experiment only 16 electrodes are used similar to the case with numerical simulations. The two immiscible liquids are placed in the phantom with a guide placed below to vary the shape of the gelatine and brine interface (Fig. 10 (a)). Opposite method is used as current injection method since it has good sensitivity at the center. Current of magnitude 10 mA is applied across the electrodes and the resulting voltage

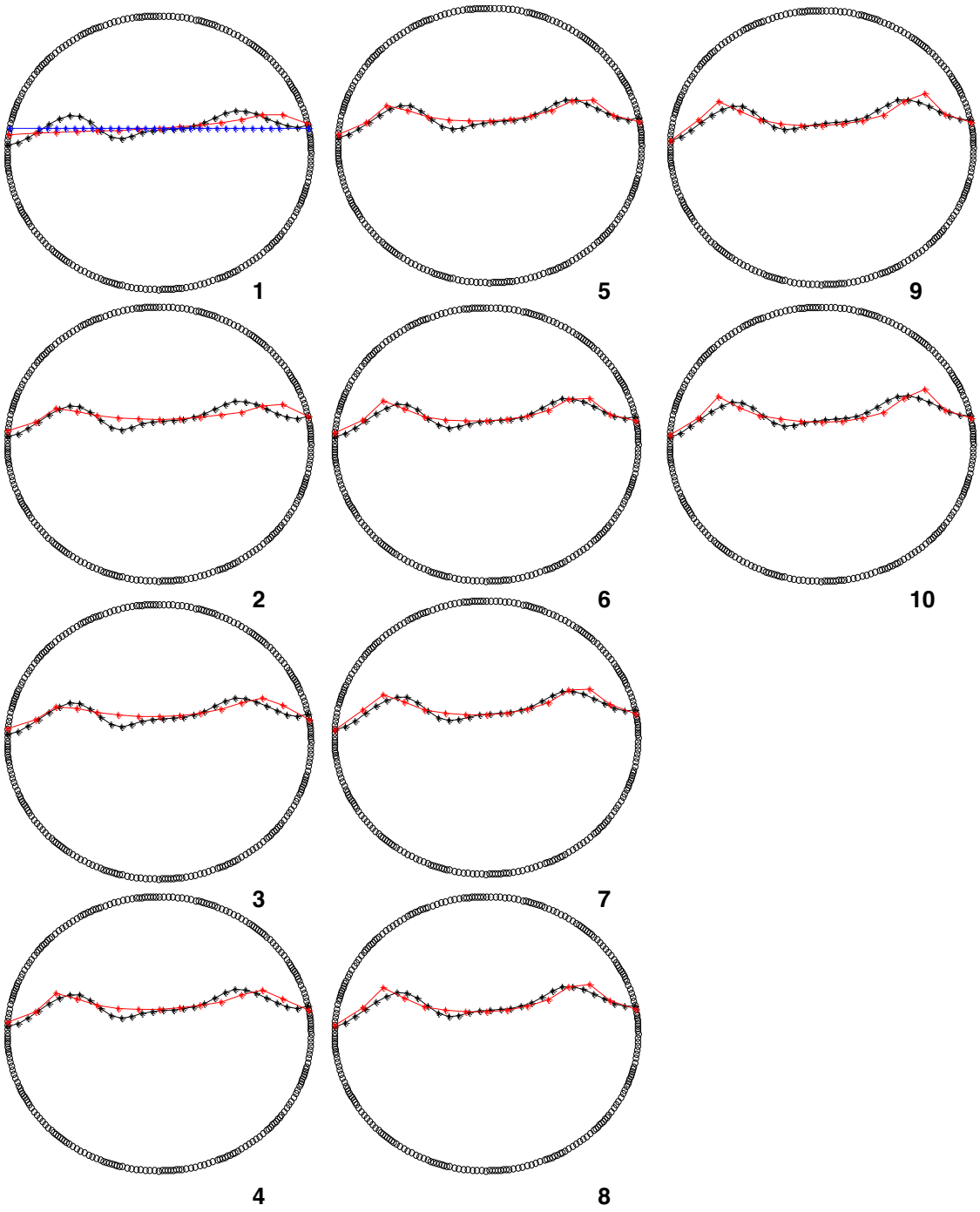


Fig. 7. Reconstructed moving interfacial boundary results with conductivity contrast 20 for numerical scenario 2. The solid black line represents the location and shape of actual boundary. The solid blue line represents the initial guess used in EKF method. The solid red line is the estimated result with proposed BEM with EKF.

measurements are recorded. The interface shape and location is varied after four current injection patterns, i.e. the interface changes two times within one frame of voltage data recorded. A total of three frames of data are considered where the interface changes six times as shown in Fig. 10(b). Experiment is performed with gelatine that has conductivity of 4.8 mS/cm and brine solution with conductivity 55.5 mS/cm. Therefore, the conductivity contrast between the modelled immiscible liquids is 11.33 i.e. $\kappa = 0.088$. The interfacial boundary initially has a smooth wavy shape and with time, the interface evolves inside the phantom as shown in Fig. 11(b). In inverse computation, for BEM boundary discretization, five segments each on electrode and gap regions

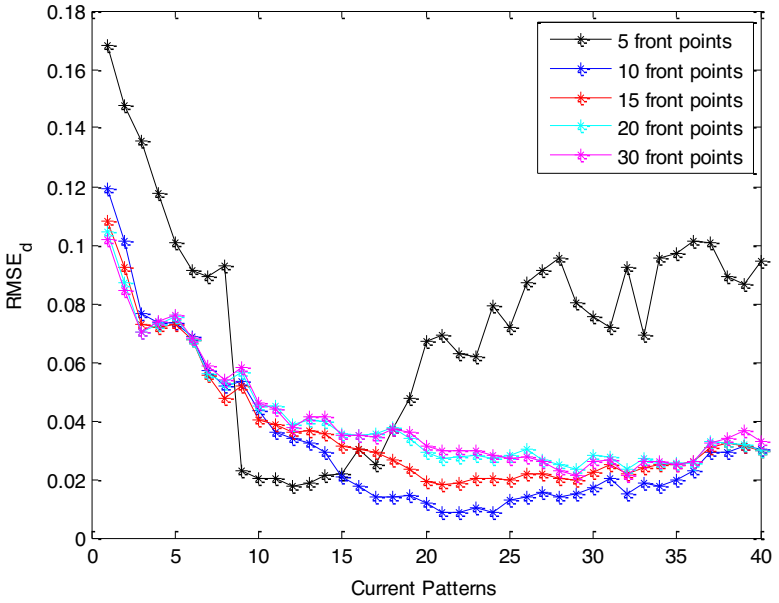


Fig. 8. Reconstruction performance of proposed method with respect to number of front points for numerical scenario 2 having conductivity contrast 20.

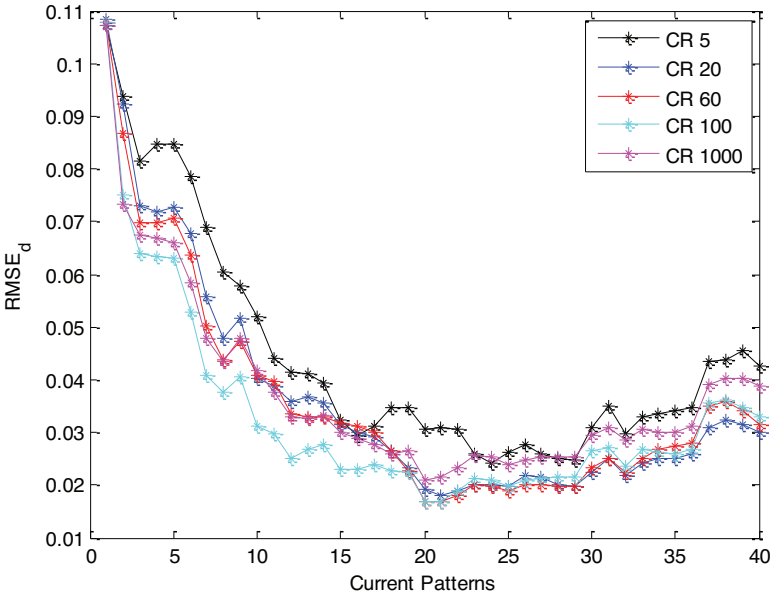


Fig. 9. Reconstruction performance of proposed method in scenario 2 having different conductivity contrast between immiscible liquids.

Table 3
Parameters used in EKF for experimental scenario.

Parameters	$\kappa = 0.088$
F	I_{10}
$\overline{Q}$	$0.02\, I_{10}$
$\overline{R}$	$30\, I_L$
$P_{0\|0}$	$0.01\, I_{10}$

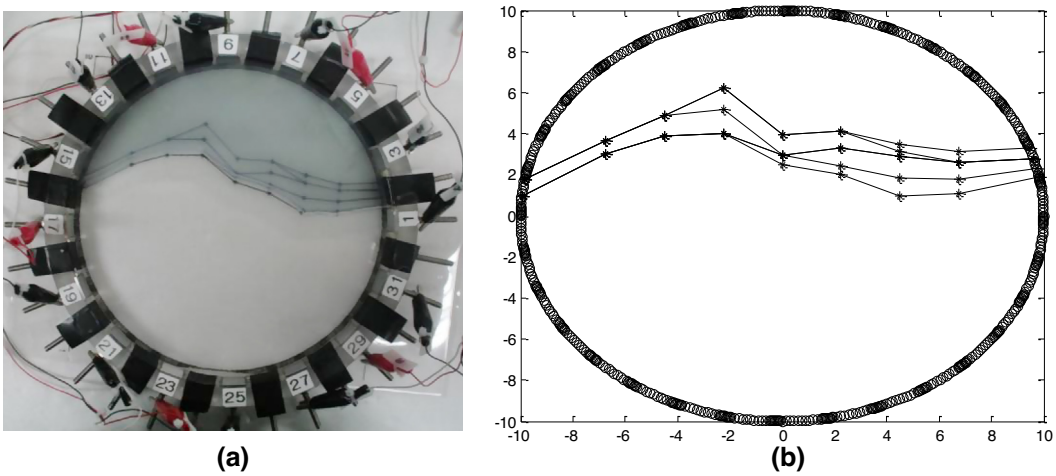


Fig. 10. Experimental studies for interfacial boundary estimation. (a) Laboratory setup for open boundary estimation using gelatin and brine solution simulated as immiscible liquids. (b) Dynamic scenario used for moving interfacial boundary experiment.

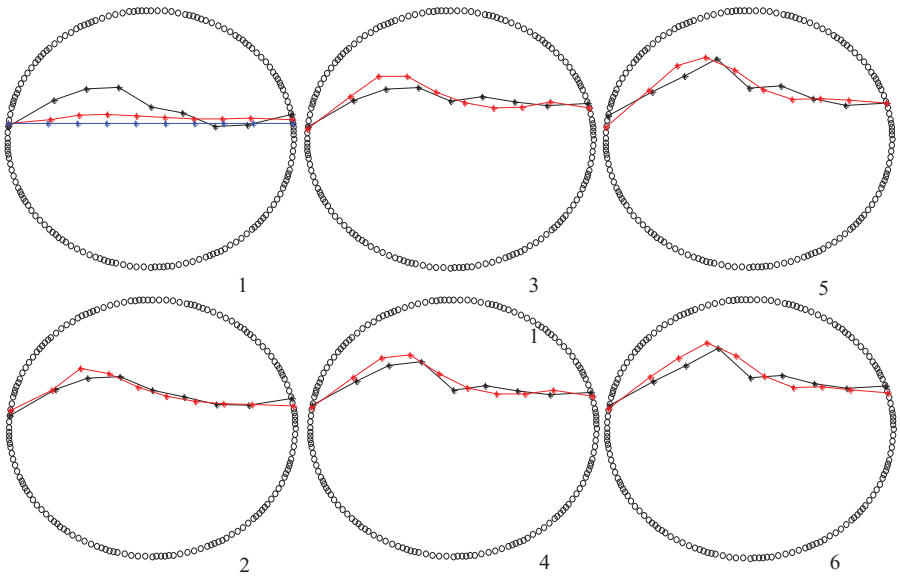


Fig. 11. Reconstructed moving interfacial boundary results with experiment data. The solid black line represents the location and shape of actual boundary. The solid blue line represents the initial guess used in EKF method. The solid red line is the estimated result with proposed BEM with EKF.

are considered such that there are total 160 segments on the outer boundary. The contact impedance of the electrodes is set to 0.001 ohm-cm. The reconstructed results for experimental data with the proposed method are shown in Fig. 11. From the results, it can be seen that the wavy gelatine-brine interfacial boundary is reconstructed with good accuracy. The interfacial boundary is represented with 10 front points and using linear interpolation. The parameters that are used in EKF setting for reconstructing the boundary parameters with experimental scenario are given in Table 3. Effect of number of front points on inverse solution is studied and the result is shown in Fig. 12. From Fig. 12, it can be seen that when the interface boundary has wavy shape, with less number of front points, the estimation error is found to be high. This is due to linear interpolation used to represent the boundary shape. As the number of front points is increased, the performance is improved but with higher number of front points ($\Lambda = 20,\ \Lambda = 30$) it was observed that the neighboring points located close to phantom centre are found to fluctuate across the actual boundary. This phenomenon has similarity with numerical simulation results that are discussed earlier. From both numerical and experimental results we can realize that 10 to 15 front points are sufficient to have an acceptable solution.

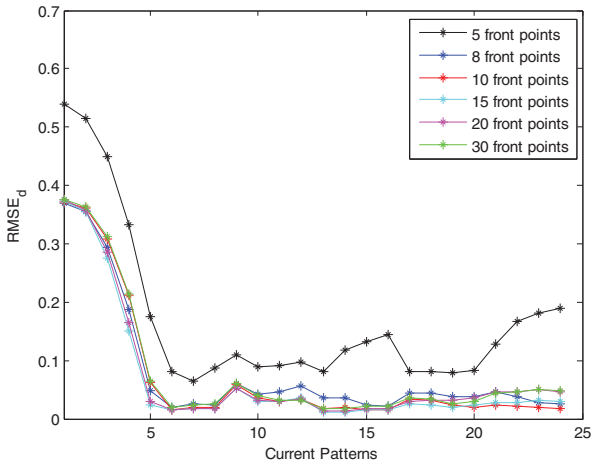


Fig. 12. Reconstruction performance of proposed method with experiment data when the number of front points is varied.

5. Conclusions

In this paper, the time-varying moving interfacial boundary between immiscible liquids is estimated using electrical resistance tomography. The interfacial boundary estimation helps in determining the liquid fraction which can play a major role in monitoring the transport of liquids through pipeline. The flow region is divided into two distinct regions separated by an open interfacial boundary. The conductivities of the immiscible liquids in the two distinct regions are assumed to be constant and known *a priori* while the unknowns are the shape and location of interfacial boundary. The boundary shape and location is parameterized using discrete front points. The forward problem for immiscible liquid flow is formulated using analytical boundary element method. The inverse problem is treated as a state estimation problem and the unknown front point variables that describe the shape of interface boundary are estimated using extended Kalman filter. The proposed method is tested with numerical scenarios in which the interfacial boundary changes its location and shape within the time to acquire full set of ERT voltage measurements. It was found that the proposed method is successful in estimating the moving interfacial boundary with good accuracy even in the presence of noise and conductivity contrast ratios up to 1000. Also, using EKF, the temporal resolution is improved by two times in scenario 1 and eight times in scenario 2. Experiments for moving interfacial boundary estimation are performed using gelatin and brine solution modeled as two immiscible liquids inside the test phantom. The results from phantom experiment show that the proposed method can work in practical conditions as well.

It is to be noted that dynamic image reconstruction depends on how well the current injection can distinguish the changes in the flow domain. Therefore, efficient data collection methods can result in improving the reconstruction performance. Also, 3D imaging would give a better picture of the actual process inside the process vessel. In modeling the forward problem using 3D BEM, analytic computation of boundary integrals for surface elements have to be computed and also singularity issue has to be addressed. The future work will be focused on finding efficient data collection method and 3D BEM formulation for shape estimation.

Acknowledgments

This work was supported by Chung-Ang University Research Grants received in 2014, Priority Research Centers Program (No. NRF-2010-0020077) through the National Research Foundation of Korea (NRF) grant funded by Ministry of Education (MOE) and Nuclear R&D Program (No. NRF-2012M2A8A4055548) through the National Research Foundation of Korea (NRF) grant funded by Ministry of Science, ICT and Future planning (MSIP)

References

[1] P. Angeli, G.F. Hewitt, Flow structure in horizontal oil-water flow, Int. J. Multiph. Flow. 26 (2000) 1117–1140.
[2] Y.V. Fairuzov, Numerical Simulation of Transient Flow of Two Immiscible Liquids in Pipeline, Am. Inst. Chem. Eng. J. 46 (2000) 1332–1339.
[3] N. Brauner, D. Moalem Maron, Flow pattern transitions in two phase liquid-liquid flow in horizontal tubes, Int. J. Multiph. Flow. 18 (1992) 123–140.
[4] F.A. Holand, R. Bragg, Fluid Flow for Chemical Engineers, Edward Arnold Publisher, London, 1995.
[5] E. Fransolet, M. Crine, P. Marchot, D. Toye, Analysis of gas holdup in bubble columns with non-Newtonian fluid using electrical resistance tomography and dynamic gas disengagement technique, Chem. Eng. Sci. 60 (2005) 6118–6123.
[6] J.G. Webster, Electrical Impedance Tomography, Adam Hilger, Bristol, 1990.
[7] D.K. Han, A. Prosperetti, A shape decomposition technique in electrical impedance tomography, J. Comput. Phys. 155 (1999) 75–95.
[8] V. Kolehmainen, A. Voutilainen, J.P. Kaipio, Estimation of non-stationary region boundaries in EIT - State estimation approach, Inverse Probl. 17 (2001) 1937–1956.
[9] O-P. Tossavainen, M. Vauhkonen, L.M. Heikkinen, T. Savolainen, Estimating shape and free surfaces with electrical impedance tomography, Meas. Sci. Technol. 15 (2004) 1402–1411.

[10] E.T. Chung, T.F. Chan, X.C. Tai, Electrical impedance tomography using level set representation and total variational regularization, J. Comput. Phys. 205 (2005) 357–372.
[11] M.C. Kim, S. Kim, K.Y. Kim, K.H. Seo, H.J. Jeon, J.H. Kim, B.Y. Choi, Estimation of phase boundary by front points method in electrical impedance tomography, Inverse Probl. Sci. Eng. 14 (2006) 455–466.
[12] A.K. Khambampati, U.Z. Ijaz, J.S. Lee, S. Kim, K.Y. Kim, Phase boundary estimation in electrical impedance tomography using Hooke and Jeeves pattern search method, Meas. Sci. Technol. 21 (2010) 035501, doi:10.1088/0957-0233/21/3/035501.
[13] V. Kolehmainen, S.R. Arridge, W.R.B. Lionheart, M. Vauhkonen, J.P. Kaipio, Recovery of region boundaries of piecewise constant coefficients of elliptic PDE from boundary data, Inverse Probl. 15 (1999) 1375–1391.
[14] O-P. Tossavainen, M. Vauhkonen, V. Kolehmainen, A three dimensional shape estimation approach for tracking of phase interfaces in sedimentation processes using electrical impedance tomography, Meas. Sci. Technol. 18 (2007) 1413–1424.
[15] J.E. Butler, R.T. Bonnecaze, Inverse method for imaging a free surface using electrical impedance tomography, Chem. Eng. Sci. 55 (2000) 1193–1204.
[16] S. Kim, U.Z. Ijaz, A.K. Khambampati, K.Y. Kim, M.C. Kim, S.I. Chung, Moving interfacial boundary estimation in stratified flows of two immiscible liquids using electrical resistance tomography, Meas. Sci. Technol. 18 (2007) 1257–1269.
[17] O-P. Tossavainen, M. Vauhkonen, V. Kolehmainen, K.Y. Kim, Tracking of moving interfaces in sedimentation processes using electrical impedance tomography, Chem. Eng. Sci. 61 (2006) 7717–7729.
[18] R. Wang, B.A. Lee, J.S. Lee, K.Y. Kim, S. Kim, Analytical estimation of liquid film thickness in two-phase annular flow using electrical resistance measurement, Appl. Math. Model. 36 (2012) 2833–2840.
[19] R. Duraiswami, K. Sarkar, G.L. Chahine, Boundary element techniques for efficient 2-D and 3-D electrical impedance tomography, Chem. Eng. Sci. 52 (1997) 2185–2196.
[20] R. Duraiswami, K. Sarkar, G.L. Chahine, Efficient 2D and 3D electrical impedance tomography using dual reciprocity boundary element techniques, Eng. Anal. Bound. Elem. 22 (1998) 13–31.
[21] M. Tarvainen, M. Vaukhonen, T. Savolainen, J.P. Kaipio, Boundary element method and internal electrodes in electrical impedance tomography, Int. J. Numer. Meth. Eng. 50 (2001) 809–824.
[22] L. Marin, L. Elliott, D.B. Ingham, D. Lesnic, The boundary element method for the numerical recovery of a circular inhomogeneity in an elliptic equation, Eng. Anal. Bound. Elem. 28 (2004) 413–419.
[23] M. Tanaka, Y. Masuda, Boundary element method applied to some inverse problems, Eng. Anal. Bound. Elem. 3 (1986) 138–143.
[24] R.G. Aykroyd, B.A. Cattle, A boundary element approach for the complete electrode model of EIT illustrated using simulated and real data, Inverse Probl. 15 (2007) 441–461.
[25] Y. Xu, F. Dong, C. Tan, Electrical resistance tomography for locating inclusions using analytical boundary element integrals and their partial derivatives, Eng. Anal. Bound. Elem. 34 (2010) 876–883.
[26] A.K. Khambampati, B.A. Lee, K.Y. Kim, S. Kim, An analytical boundary element integral approach to track the boundary of a moving cavity using electrical impedance tomography, Meas. Sci. Technol. 23 (2012) 035401, doi:10.1088/0957-0233/23/3/035401.
[27] S. Ren, F. Dong, C. Tan, Y. Xu, A boundary element approach to estimate the free surface in stratified two-phase flow, Meas. Sci. Technol. 23 (2012) 105401, doi:10.1088/0957-0233/23/10/105401.
[28] A.K. Khambampati, Y.J. Hong, K.Y. Kim, S. Kim, Estimation of open boundary between two immiscible liquids using analytical boundary element integral approach, Chem. Eng. Sci. 95 (2013) 161–173.
[29] K.S. Cheng, D. Isaacson, J.C. Newell, D.G. Gisser, Electrode models for electric current computed tomography, IEEE Trans. Biomed. Eng. 36 (1989) 918–924.
[30] E. Somersalo, M. Cheney, D. Isaacson, Existence and uniqueness for electrode models for electric current computed tomography, SIAM J. Appl. Math. 52 (1992) 1023–1040.
[31] W.T. Ang, A Beginner's Course in Boundary Element Methods, Universal-Publishers, 2007.
[32] M. Fratantonio, JJ. Rencis, Exact boundary element integrations for two dimensional Laplace equation, Eng. Anal. Bound. Elem. 24 (2000) 325–342.
[33] W. Tang, R. Fenner, Analytical integral algorithm applied to boundary layer effect and thin body effect in BEM for anisotropic potential problems, Appl. Math. Model. 29 (2005) 1073–1099.
[34] C.A. Brebbia, J. Dominguez, Boundary Elements, An Introductory Course, second ed., Comp. Mech. Publicatons and Mc Graw-Hill Book Co., Southampton and Boston, 1992.
[35] X. Zhang, X. Zhang, Exact integration in the boundary element method for two-dimensional elastostatic problems, Eng. Anal. Bound. Elem. 27 (2003) 987–997.
[36] M. Dehghan, H. Hosseinzadeh, Calculation of 2D singular and near singular integrals of boundary elements method based on the complex space, Appl. Math. Model. 36 (2012) 545–560.
[37] K.Y. Kim, B.S. Kim, M.C. Kim, Y.J Lee, M. Vauhkonen, Image reconstruction in time varying electrical impedance tomography based on the extended Kalman filter, Meas. Sci. Technol. 12 (2001) 1032–1039.